BULLETIN OF THE POLISH ACADEMY OF SCIENCES
TECHNICAL SCIENCES, Vol. 70(1), 2022, Article number: e140437
DOI: 10.24425/bpasts.2022.140437

The effect of selected nanoparticles on rheological properties of human blood

Urszula MICHALCZUK, Rafał PRZEKOP*, and Arkadiusz MOSKAL

Warsaw University of Technology, Faculty of Chemical and Process Engineering, ul. Waryńskiego 1, 00-645 Warsaw, Poland

Abstract. The aim of the study was to determine the influence of selected nanoparticles, namely diesel exhaust particles, Arizona test dust, silver and gold on the rheology of human blood. The rheological properties of human blood were determined with the use of a modular rheometer, at two various temperatures, namely 36.6°C and 40°C. Experimental results were used to calculate the constants in blood constitutive equations. The considered models were power-law, Casson and Cross ones. The obtained results demonstrate that the presence of different nanoparticles in the blood may have different effect on its apparent viscosity depending on the type of particles and shear rate.

Key words: blood; nanoparticles; non-Newtonian rheology.

1. INTRODUCTION

Global emission and production of nanoparticles including fibrous materials are significantly growing causes the accumulation into the natural environment [1, 2]. Consequently, nanoparticles are present in food [3], drinking water [4] or human lungs [5]. Due to their size, submicron particles are easily inhaled (particles with a diameter below 5 μm are known as a respirable fraction) and have the ability to penetrate the deepest region of the respiratory system–bronchioles and alveoli. Inhaled nanoparticles can easily cross the alveolar-capillary barrier and directly affect the cardiovascular system [6–8]. On the other hand, inhalation is used as an effective way of nanosized drugs delivery [9]. Number of theoretical studies on the nanoparticles bahaviour in blood were published recently [10–13]. All of them treat nanoparticles suspension in blood as a nanofluid. However, blood should be considered as a suspension of elastic particulate cells in a liquid (plasma) [14]. The weight composition of the continuous phase of human blood, plasma, is roughly 91% water, 7% proteins and 2% inorganic solutes and other organic substances [15]. Plasma may be considered a Newtonian fluid with a viscosity of about 1.2 mPas at 37°C [16]. The dispersed phase of blood consists of erythrocytes or red blood cells (RBCs), leukocytes or white blood cells (WBCs), and platelets. RBCs are the predominant cell type of blood and represent cellular volume fraction more than 99% [17]. The RBCs volume fraction is called the hematocrit and its typical range is around 0.45 in adult humans [16]. RBCs have a biconcave discoid shape. Blood rheology is strongly affected by the aggregatable and deformable properties of the red RBCs. RBCs aggregation leads to the increase of blood viscosity at low shear rates. The rate of RBCs aggregation is a function of their concentration and shear rate [18]. When the shear rate tends to zero, RBCs form one big cluster, which performs like a solid body. These aggregates are built from smaller units known as rouleaux. As the shear rate increases, the average number of RBCs in each rouleaux decreases and finally the rouleaux are broken up into individual cells that tend to become elongated and line up with the streamlines [19]. Thus mechanical properties of RBCs and their ability to form clusters are crucial for the blood's rheology. The influence of diesel exhaust particles on red blood cells was experimentally studied [20]. However, no comprehensive experimental studies on the relation between nanoparticles' presence and blood rheology were published so far. In this study we investigate the effect of selected nanoparticles on the rheological properties of human blood.

2. MATERIALS

2.1. Blood

In the research the expired blood from blood donation centre was used. The blood from blood donation centre contains 70 ml of CPDA-1 anticoagulant per 450 ml of blood.

2.2. Arizona test dust (nominal 0–3 μm, Powder Technology INC, USA)

The Arizona test dust (ATD) is commonly used in many applications such as water and air filter performance testing. It is obtained in the four-step process from raw dust from Salt River Valley (Arizona). Therefore, we assumed that Arizona dust might be a good equivalent of natural dust. The chemical composition of Arizona dust based on the safety data sheet is shown in Table 1. The size distribution in water suspension was obtained using the Zetasizer (Malvern, UK). Figure 2(A) presents the SEM image of Arizona dust.

*e-mail: rafal.przekop@pw.edu.pl

Manuscript submitted 2021-06-30, revised 2021-09-06, initially accepted for publication 2021-10-14, published in February 2022.

Table 1
Chemical composition of Arizona dust

Spiece	Mass fraction [%]
Silica dioxide	68.0–78.0
Aluminium dioxide	10.0–15.0
Iron (III) oxide	2.0–5.0
Calcium oxide	2.0–5.0
Potassium chloride	2.0–5.0
Sodium oxide	2.0–4.0
Magnesium oxide	1.0–2.0
Titanium oxide	0.5–1.0

2.3. Diesel exhaust particles (DEP)

DEP soot aggregates were obtained by combustion of fuel VERVA ON (PKN Orlen, min. CN = 55) in a diesel engine with four cylinders and a capacity of 2399 cm^3 (Mercedes). The engine had no filter or catalyst. The engine was idling and its rotation speed was about 800 rpm. In order to deposit the DEP aggregates, a special chamber (Fig. 3) was connected to the engine exhaust pipe. Inside, Petri dishes were placed on which aggregates of soot were deposited. The size distribution of DEP is presented in Fig. 1. Figure 2(B) shows the SEM image of DEPs. The particle size distribution was measured the same way as for Arizona dust.

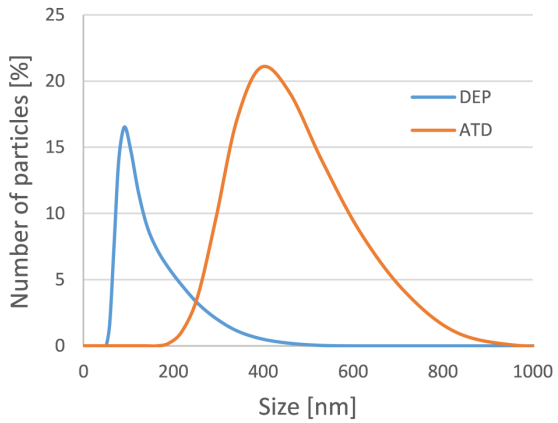

Fig. 1. Size distribution of diesel exhaust particles (DEP) and Arizona test dust (ATD)

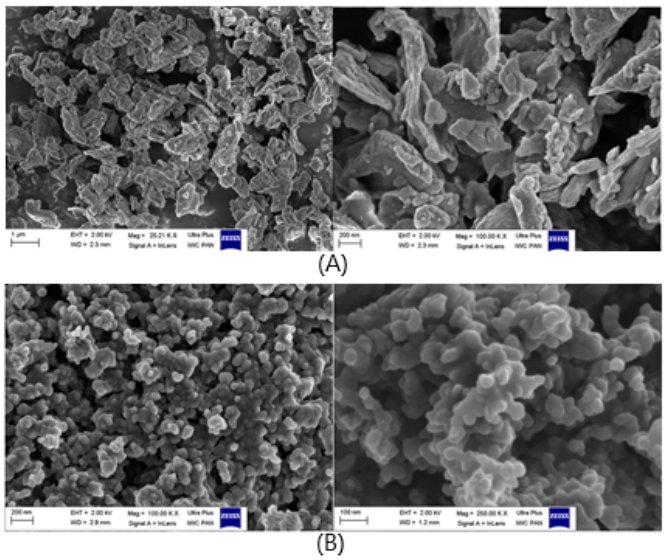

Fig. 2. SEM pictures of (A) diesel exhaust particles (DEP) and (B) Arizona test dust (ATD)

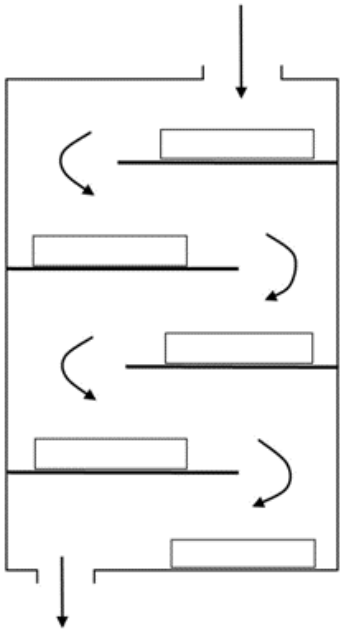

Fig. 3. Chamber for diesel exhaust particle collection

2.4. Silver and gold nanoparticles

Suspensions of monodisperse silver (10 and 40 nm, referred as S10 and S40, respectively) and gold (5 and 50 nm, referred as G5 and G50, respectively) nanoparticles used in the experiments were manufactured by Sigma Aldrich. The concentration of silver nanoparticles was 0.2 mg/ml, while the number concentration of gold nanoparticles was $5.5 \cdot 10^{13}$ and $3.5 \cdot 10^{10}$ for 5 nm and 50 nm, respectively.

3. BLOOD RHEOLOGY

At higher shear rates the Newtonian model which assumes the constant value of viscosity equal to 0.0035 Pas may be used for the description of human blood's rheology. At lower shear rates diverse forms of non-Newtonian constitutive equations, characterizing shear thinning behavior of blood caused by RBCs dispersion and deformation, are applied. The power-law [21], Casson [22] and Cross [23] models are frequently used non-Newtonian ones. The power-law model of blood viscosity takes the form:

$$\mu = k\dot{\gamma}^{n-1}, \tag{1}$$

where μ is viscosity, k is the flow consistency index, $\dot{\gamma}$ is shear rate and n is the power-law index. The lower value of the power-law index, n, indicates the stronger shear thinning behavior of a fluid. The constants of the model depend on the concentration

of both, dissolved and dissoluted, constituents of blood. It was experimentally shown that blood at rest requires yield stress to start flowing. The power-law does not consider this specific behavior, however, the Casson model, takes into account this property of blood and is given by:

$$\mu = \frac{\tau_0}{\dot{\gamma}} + 2\sqrt{\frac{\tau_0 \eta}{\dot{\gamma}}} + \eta, \tag{2}$$

where τ_0 is the yield stress and η is the Casson rheological constant. The third non-Newtonian model considered in this article is the Cross model described by the equation:

$$\mu = \mu_\infty + \frac{\mu_0 - \mu_\infty}{1 + (\lambda \dot{\gamma})^n}, \tag{3}$$

where μ_0 and μ_∞ are the limiting viscosities at zero and infinite shear rates, respectively, λ is the relaxation time constant and n is the power-law index. The inversion of relaxation time constant is called critical shear rate and describes the maximum shear rate at which fluid viscosity may be assumed as equal to μ_0. The power-law index controls the slope of the curve in the power-law region. The values of the parameters for blood for the constitutive equation discussed above are presented in Table 2.

Table 2
Constants in blood rheorogical models

Parameter	Value		
	at 36.6°C [24]	at 36.6°C (this work)	at 40°C (this work)
Flow consistency index, k [Pas^n]	0.017	0.019	0.025
Power law index, n [–]	0.708	0.62	0.61
Yield stress, τ_0 [Pa]	0.05	0.026	0.059
Casson's rheological constant η [Pas]	0.0035	0.0031	0.0035
Zero shear rate viscosity limit μ_0 [Pas]	0.056	0.045	0.079
Infinite shear rate viscosity limit μ_∞ [Pas]	0.00345	0.00333	0.00393
Relaxation time constant, λ [s]	1.007	1.003	1.003
Power law index in Cross model, n [–]	1.028	1.482	1.561

4. METHODS

We have investigated the rheological properties of blood with the addition of nanoparticles. The Arizona dust and DEPs were initially suspended standard saline (0.9% NaCl) in the concentration of 6 mg/ml and added to the blood to obtain a concentration 0.06 mg/ml. The saline for DEPs have contained Tween 80 (0.01%) to protect particles from aggregation [20]. Additionally, the sample with DEPs was sonicated in an ultrasonic cleaner (RK 106, Bandelin Sonorex) for 1 hour. The silver and gold nanoparticles were soluted to obtain the concentration 20 times lower than the initial one what gives 0.01 mg/ml for silver and 0.0035 mg/ml and 0.0022 mg/ml for 5 and 50 nm gold nanoparticles, respectively. The prepared samples were incubated for 2 hours at the temperature of measurement in a water bath. The dependence of viscosity as a function of shear rate was examined with a modular rheometer (MCR102, Anton Paar, Austria) equipped with a Peltier system in a plate-plate system for a 1-mm-wide gap. For the assumed value of shear rate, the shear stress was measured from which the value of apparent viscosity may be easily calculated. The tests were carried out at two temperatures: 36.6°C and 40°C, what corresponds to the case healthy and ill human. The rheological properties of blood with standard saline addition were measured as the reference value.

5. RESULTS AND DISCUSSION

The experiments were carried out for the shear rates from the range 0.1–100 s^{-1}. Shear stresses from the shear rate range 10–200 s^{-1} are typical for human veins [25]. Figures 4 and 5 present the viscosity of blood as a function of shear rate for the temperatures 36.6°C and 40°C, respectively. One can observe that apparent viscosity for the shear rate $\dot{\gamma} > 50$ s^{-1} (36.6°C) can be assumed constant what is consistent with other experimental studies [26]. The limiting value of blood's apparent viscosity (3.33 mPas) is also in good agreement with data available in literature [24]. We have used our data to calculate the constants for 3 models of blood viscosity and compare them to the values presented by available in the literature in Table 1. The constants were calculated from experimental data by the least-squares method. The slight differences may be explained by several reasons. Blood used in our experiment was after the expiration date, the coagulant was added, so the apparent viscosity at low shear rates and yield stress were lower. Additionally, we were not aware of the exact value of the hematocrit of the blood used in the experiment and additionally it was dissoluted by normal saline. The differences between the values of the fit parameters of the 3 models may occur because the blood

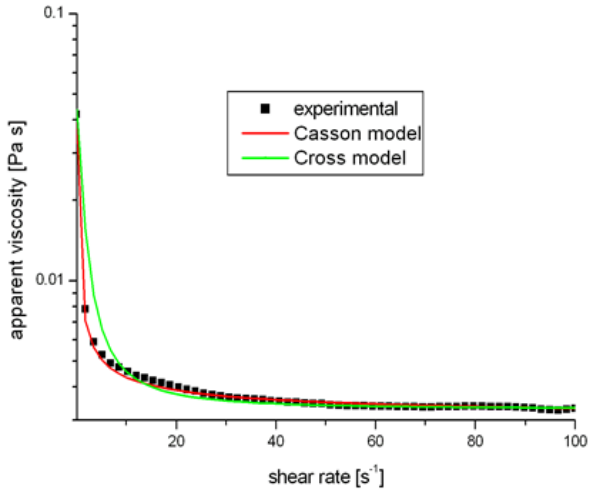

Fig. 4. Apparent viscosity of blood at 36.6°C

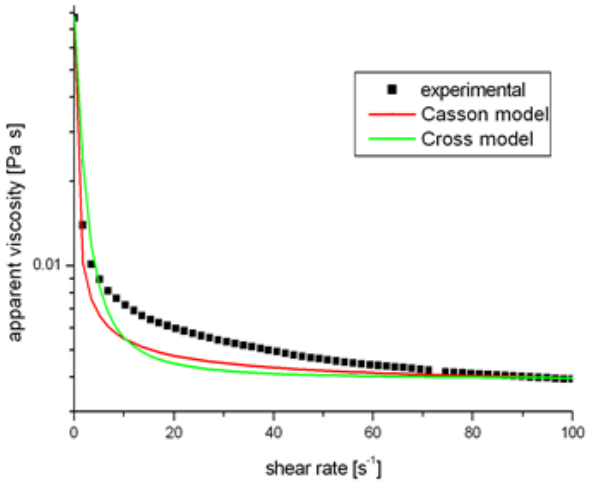

Fig. 5. Apparent viscosity of blood at 40°C

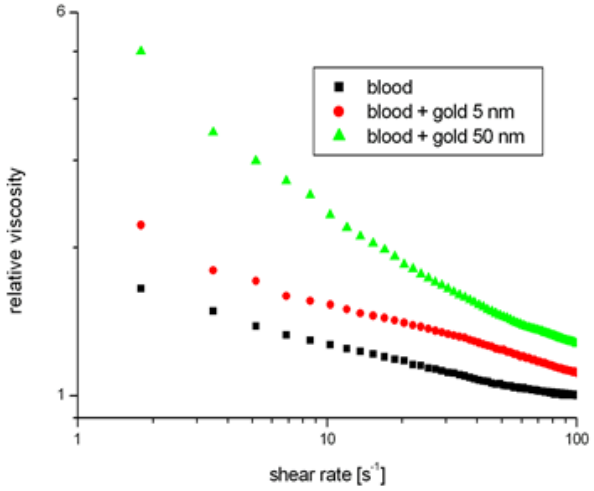

Fig. 7. Relative viscosity of blood with gold nanoparticles at 36.6°C

viscosity is also influenced by other factors: age and sex of the patient, possible diseases or treatments followed, time of day and area of the body from which the blood was collected. Figure 4 shows that Casson and Cross models fit the experimental data for the whole range of share rates used in our study in the temperature of 36.6°C. For the blood in the temperature of 40°C (Fig. 5) the values of apparent viscosity are underestimated by both models for the share rates from the range 20-70 s^{-1}. Figures 6–9 show the relative apparent viscosity for the nanoparticles suspensions in blood at the temperature 36.6°C, while Figs. 10–13 show the same relation at the temperature 40°C. The relative apparent viscosity was defined as the rate of apparent viscosity to the infinite shear rate limit for the blood with saline under the same temperature. The values of zero and infinite shear limits and yield stress were estimated for all the solutions at the temperatures of 36.6°C and 40°C by the regression of experimental date to Casson and Cross equations. Their relative values to the value calculated for blood with saline are summarized in Tables 3 and 4. Additionally, the square of the

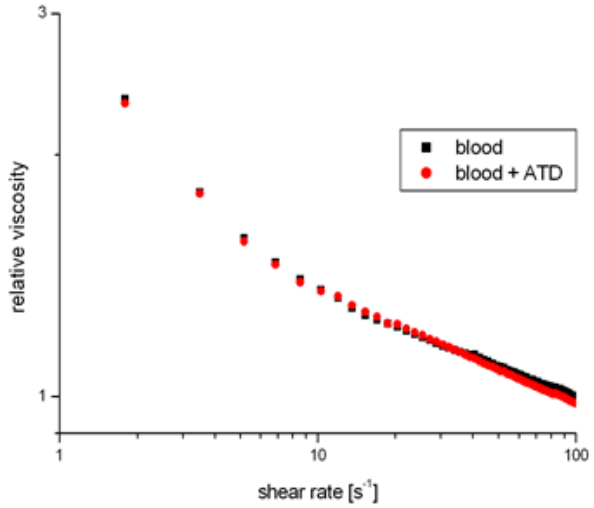

Fig. 8. Relative viscosity of blood with Arizona dust particles at 36.6°C

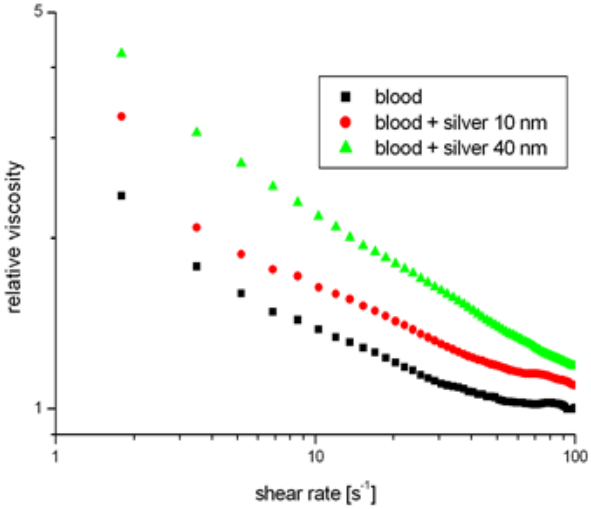

Fig. 6. Relative viscosity of blood with silver nanoparticles at 36.6°C

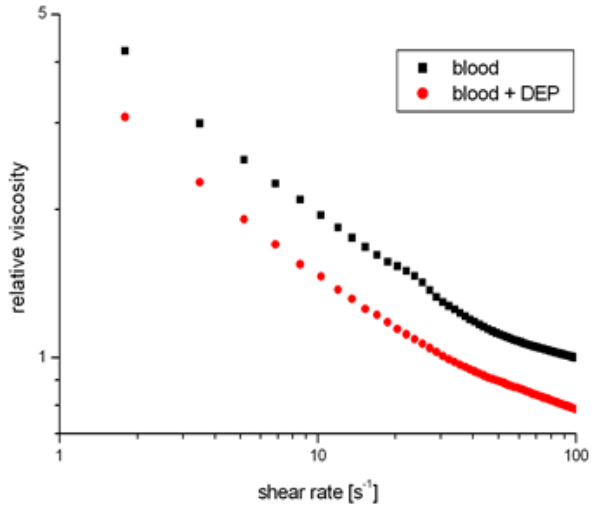

Fig. 9. Relative viscosity of blood with diesel exhaust particles at 36.6°C

Table 3
Relative values of constants in blood rheorogical models at 36.6°C

Parameter	S10	S40	G5	G50	DEP	ATD
Zero viscosity	1.167	1.810	1.009	1.833	0.665	1.028
Infinite viscosity	1.093	1.180	1.006	1.072	0.789	0.981
Yield stress	1.005	1.082	1.003	1.084	0.832	1.002

Table 4
Relative values of constants in blood rheorogical models at 40°C

Parameter	S10	S40	G5	G50	DEP	ATD
Zero viscosity	2.729	1.341	1.673	3.223	0.642	0.962
Infinite viscosity	1.098	1.291	1.109	1.272	0.874	0.983
Yield stress	1.626	2.041	1.023	1.935	0.811	0.958

correlation coefficients, R^2, for the linearized realtions between the apparent viscosity and shear rate were calculated. The linearized relations between the apparent viscosity and shear rate can be written as follows:

$$\ln(\mu) \sim \ln(\dot{\gamma}) \tag{4}$$

for all the considered models. The square of the correlation coefficients for all the investigated cases are summarized in Tables 5 and 6 for the temperatures of 36.6°C and 40°C, respectively. The values of R^2 show that the Casson model fits the experimental data with the best accuracy. The presence of silver and gold nanoparticles increases the apparent viscosity of the blood. The effect is more visible at 40°C. Moreover, one can observe that larger nanoparticles (50 and 40 nm for gold and silver, respectively) have a stronger influence on the blood viscosity than the smaller ones. There are two potential mechanisms that may lead to the increase of blood viscosity. The first hypothesis is that presence of the nanoparticles attached to the surface

Table 5
Values of the square of the coefficient of correlation R^2 at 36.6°C

model	power-law	Cross	Casson
blood	0.883	0.925	0.937
S10	0.854	0.911	0.923
S40	0.870	0.918	0.927
G5	0.873	0.921	0.929
G50	0.875	0.916	0.924
DEP	0.874	0.921	0.931
ATD	0.882	0.925	0.938

Table 6
Values of the square of the coefficient of correlation R^2 at 40°C

model	power-law	Cross	Casson
blood	0781	0.825	0.838
S10	0.773	0.811	0.824
S40	0.765	0.819	0.828
G5	0.780	0.822	0.827
G50	0.769	0.817	0.824
DEP	0.733	0.790	0.803
ATD	0.725	0.785	0.792

of erythrocytes may increase the value of adhesion force acting between them. The other potential mechanism of the increase of blood viscosity is the stiffening of the red blood cell membrane by the presence of attached nanoparticles. Contrary to the presence of metal nanoparticles, the presence of DEPs leads to a significant decrease of the blood's apparent viscosity. The effect is quite similar regardless of the temperature. It's probably caused by the destruction of red blood cells membranes by the soot particles. Our hypotheses are consistent with the research on the

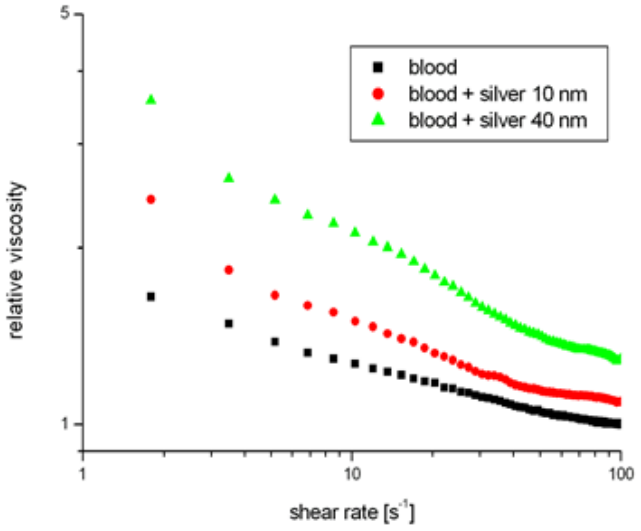

Fig. 10. Relative viscosity of blood with silver nanoparticles at 40°C

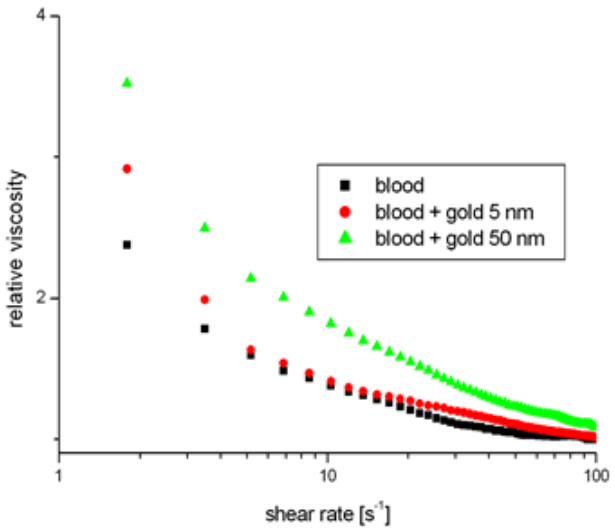

Fig. 11. Relative viscosity of blood with gold nanoparticles at 40°C

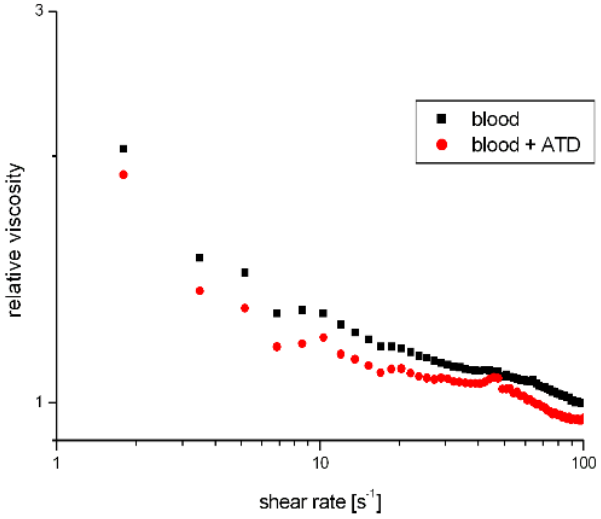

Fig. 12. Relative viscosity of blood with arizona dust particles at 40°C

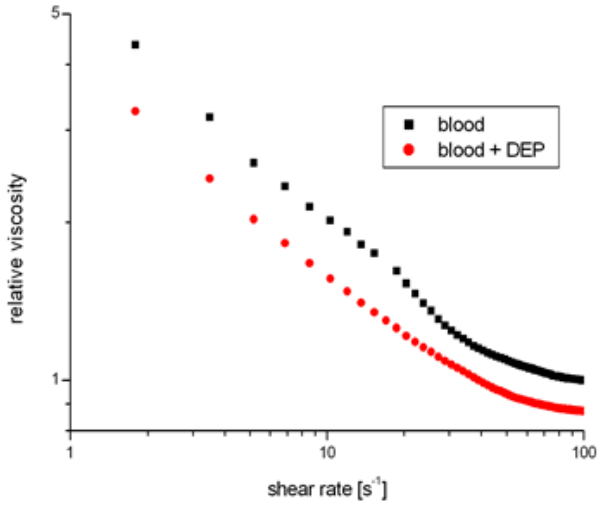

Fig. 13. Relative viscosity of blood with diesel exhaust particles at 40°C

influence of some dieseases on the blood's rheology and mechanical properties of RBCs [14, 27, 28]. As a future work, we aim to investigate theoretically the effect of nanoparticles' presence on the RBCs surfaces on their mechanical properties using molecular dynamics method. For Arizona dust no effect on the blood rheology was observed for the temperature of 36.6°C and a slight decrease of apparent viscosity was observed at 40°C. We can assume that Arizona dust has no tendency to attach to the RBCs' surfaces. As one can see in Figs. 1 and 2 Arizona dust particles have smoother edges than DEPs so they may not cause RBCs' membranes destruction at 36.6°C. However, the mechanical resistance of the erythrocytes decreases with the temperature, what may lead to the spontaneous disintegration at the temperature of 45°C [29] and the presence of Arizona dust particles may promote the process in the lower temperature. Figure 14 shows the SEM pictures of erythrocytes from different samples. One can observe the qualitative differences in the surface structure of red blood cells related to the addition of nanoparticles.

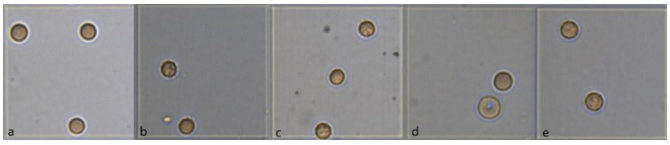

Fig. 14. SEM pictures of red blood cells: a) pure blood, b) Arizona dust, c) diesel exhaust particles, d) silver 5 nm, e) gold 10 nm

6. CONCLUSIONS

The investigations presented in this paper show that the presence of nanoparticles in the blood affects its viscosity in various ways. Silver and gold nanoparticles increase, while others decrease the blood viscosity – ATD at 40°C, DEP), which can have repercussions on health. Thus, the increase in blood viscosity can cause a reduction in cardiac output and an increase in peripheral resistance, resulting in an increase in blood pressure in conditions of difficult circulation that requires a much increased mechanical effort [30], hematological disorders [31], heart failure [32], neurological disorders [33], risk of ischemic stroke [34]. Decreased blood viscosity has the effect of the danger of bleeding, especially in conditions of a patient with a fever [35].

ACKNOWLEDGEMENTS

This work was sponsored by Warsaw University of Technology under the grant from the Council of Scientific Discipline: Chemical Engineering.

REFERENCES

[1] C.-L. Myung and S. Park, "Exhaust nanoparticle emissions from internal combustion engines: A review," *Int. J. Automotive Technol.*, vol. 13, p. 9, 2011, doi: 10.1007/s12239-012-0002-y.

[2] T. Rönkkö and H. Timonen, "Overview of sources and characteristics of nanoparticles in urban traffic-influenced areas," *J. Alzheimer's Dis.*, vol. 72, pp. 15–28, 2019, doi: 10.3233/JAD-190170.

[3] B. Naseer, G. Srivastava, O. Qadri, S. Faridi, R. Ul Islam, and K. Younis, "Importance and health hazards of nanoparticles used in the food industry," *Nanotechnol. Rev.*, vol. 7, pp. 623–641, 2018, doi: 10.1515/ntrev-2018-0076.

[4] K. Tiede *et al.*, "How important is drinking water exposure for the risks of engineered nanoparticles to consumers?" *Nanotoxicology*, vol. 10, pp. 102–110, 2016, doi: 10.3109/17435390.2015.10228.

[5] A. Penconek and A. Moskal, "Deposition of diesel exhaust particles from various fuels in a cast of human respiratory system under two breathing patterns," *J. Aerosol Sci.*, vol. 63, pp. 48–59, 2013, doi: 10.1016/j.jaerosci.2013.04.008.

[6] A. Nemmar, M. Hoylaerts, P. Hoet, and B. Nemery, "Possible mechanisms of the cardiovascular effects of inhaled particles: systemic translocation and prothrombotic effects," *Toxicol. Lett.*, vol. 149, pp. 243–253, 2004, doi: 10.1159/000430315.

[7] J. Vermylen, A. Nemmar, B. Nemery, and M. Hoylaert, "Ambient air pollution and acute myocardial infarction," *J. Thromb. Haemost.*, vol. 3, pp. 1955–1961, 2005, doi: 10.1111/j.1538-7836.2005.01471.x.

[8] R. Brook *et al.*, "Particulate matter air pollution and cardiovascular disease. An update to the scientific statement from the American Heart Association," *Circulation*, vol. 121, pp. 2331–2378, 2010, doi: 10.1161/CIR.0b013e3181dbece1.

[9] T. Sosnowski, "Nanosized and Nanostructured Particles in Pulmonary Drug Delivery," *J. Nanosci. Nanotechnol.*, vol. 5, pp. 3476–3487, 2015, doi: 10.1108/HFF-12-2019-0910.

[10] J. Prakash, D. Tripathi, A. Tiwari, S. Dait, and R. Ellahi, "Thermal, microrotation, electromagnetic field and nanoparticle shape effects on Cu-CuO/blood flow in microvascular vessels," *Symmetry*, vol. 11, p. 868, 2019, doi: 10.3390/sym11070868.

[11] D. Tripathi, J. Prakash, A. Tiwari, and R. Ellahi, "Thermal, microrotation, electromagnetic field and nanoparticle shape effects on Cu-CuO/blood flow in microvascular vessels," *Microvasc. Res.*, vol. 132, p. 104065, 2020, doi: 10.1016/j.mvr.2020.104065.

[12] A. Elelamy, N. Elgazery, and R. Ellahi, "Blood flow of MHD non-Newtonian nanofluid with heat transfer and slip effects: Application of bacterial growth in heart valve," *Int. J. Numer. Methods Heat Fluid Flow*, vol. 30, pp. 4883–4908, 2020, doi: 10.1166/jnn.2015.9863.

[13] M. Bhatti, M. Marin, A. Zeeshan, R. Ellahi, and S. Abdelsalam, "Swimming of Motile Gyrotactic Microorganisms and Nanoparticles in Blood Flow Through Anisotropically Tapered Arteries," *Front. Phys.*, vol. 8, p. 95, 2020, doi: 10.3389/fphy.2020.00095.

[14] E. Nader *et al.*, "Blood Rheology: Key Parameters, Impact on Blood Flow, Role in Sickle Cell Disease and Effects of Exercise," *Front. Physiol.*, vol. 10, p. 1329, 2019, doi: 10.3389/fphys.2019.01329.

[15] J. Mazumdar, *Biofluid Mechanics*. Singapore: World Scientific, 1992.

[16] R. Pal, "Rheology of concentrated suspensions of deformable elastic particles such as human erythrocytes," *J. Biomech.*, vol. 36, pp. 981–989, 2003, doi: 10.1016/S0021-9290(03)00067-8.

[17] C. Picart, J. Piau, H. Galliard, and P. Carpentier, "Blood low shear rate rheometry: influence of fibrinogen level and hematocrit on slip and migrational effects," *Biorheology*, vol. 35, pp. 335–353, 1998, doi: 10.1016/S0006-355X(99)80015-8.

[18] A. Zydney, "A constitutive equation for the viscosity of stored red cell suspensions: Effect of hematocrit, shear rate, and suspending phase," *J. Rheol.*, vol. 35, pp. 1639–1680, 1991, doi: 10.1122/1.550249.

[19] J. Barber, J. Alberding, J. Restrepo, and T. Secomb, "Simulated two-dimensional red blood cell motion, deformation, and partitioning in microvessel bifurcations," *Ann. Biomed. Eng.*, vol. 36, pp. 1690–1698, 2008, doi: 10.1007/s10439-008-9546-4.

[20] A. Nemmar, S. Zia, D. Subramaniyan, I. Al-Amri, M. Al-Kindi, and B. Ali, "Interaction of Diesel Exhaust Particles with Human, Rat and Mouse Erythrocytes in Vitro," *Cell. Physiol. Biochem.*, vol. 29, pp. 163–170, 2012, doi: 10.1159/000337597.

[21] M. Hussain, S. Kar, and R. Puniyani, "Relationship between power law coefficients and major blood constituents affecting the whole blood viscosity," *J. Biosci.*, vol. 24, pp. 329–337, 1999, doi: 10.1007/BF02941247.

[22] P. Neofytou, "Comparison of blood rheological models for physiological flow simulation," *Biorheology*, vol. 41, pp. 693–714, 2004.

[23] M. Gallagher, R. Wain, S. Dari, J. Whitty, and D. Smith, "Non-identifiability of parameters for a class of shear-thinning rheological models, with implications for haematological fluid dynamics," *J. Biomech.*, vol. 85, pp. 230–238, 2019, doi: 10.1016/j.jbiomech.2019.01.036.

[24] S. Shewaferaw, S. Shibeshi, and W. Collins, "The Rheology of Blood Flow in a Branched Arterial System," *Appl. Rheol.*, vol. 15, pp. 398–405, 2005, doi: 10.1901/jaba.2005.15-398.

[25] X. Shi *et al.*, "Effects of different shear rates on the attachment and detachment of platelet thrombi," *Mol. Med. Rep.*, vol. 13, pp. 2447–2456, 2016, doi: 10.3892/mmr.2016.4825.

[26] Y. Cho, J. Cho, and R. Rosenson, "Endothelial Shear Stress and Blood Viscosity in Peripheral Arterial Disease," *Curr. Atheroscler. Rep.*, vol. 16, p. 404, 2014, doi: 10.1007/s11883-014-0404-6.

[27] J. Czepiel *et al.*, "Rheological properties of erythrocytes in patients infected with Clostridium difficile," *Adv. Hyg. Exp. Med.*, vol. 68, pp. 1397–1405, 2014, doi: 10.5604/17322693.1130558.

[28] O. Baskurt, "Pathophysiological Significance of Blood Rheology," *Turk. J. Med. Sci.*, vol. 33, pp. 347–355, 2003.

[29] N. Gershfeld and M. Murayama, "Thermal Instability of Red Blood Cell Membrane Bilayers: Temperature Dependence of Hemolysis," *J. Membr. Biol.*, vol. 101, pp. 67–72, 1988.

[30] R. Devereux, D. Case, M. Alderman, T. Pickering, S. Chien, and J. Laragh, "Possible role of increased blood viscosity in the hemodynamics of systemic hypertension," *Am. J. Cardiol.*, vol. 85, pp. 1265–1268, 2000, doi: 10.1016/S0002-9149(00)00744-X.

[31] X. Li, H. Li, H.-Y. Chang, G. Lykotrafitis, and G. Karniadaki, "Computational Biomechanics of Human Red Blood Cells in Hematological Disorders," *J. Biomech. Eng.*, vol. 139, p. 021008, 2017, doi: 10.1115/1.4035120.

[32] R. Gal *et al.*, "Hemorheological Alterations in Patients with Heart Failure with Reduced Ejection Fraction Treated by Resveratrol," *Cardiovasc. Ther.*, vol. 2020, p. 7262474, 2020, doi: 10.1155/2020/7262474.

[33] M. Akcaboy, B. Nazliel, T. Goktas, S. Kula, B. Celik, and N. Buyan, "Whole blood viscosity and cerebral blood flow velocities in obese hypertensive or obese normotensive adolescents," *J. Pediatr. Endocrinol. Metabol.*, vol. 31, pp. 275–281, 2018, doi: 10.1515/jpem-2017-0436.

[34] A. Rasyid, S. Harris, M. Kurniawan, T. Mesiano, and R. Hidayat, "Fibrinogen and LDL Influence on Blood Viscosity and Outcome of Acute Ischemic Stroke Patients in Indonesia," *Ann. Neurosci.*, vol. 26, pp. 30–34, 2019, doi: 10.1177/0972753119900630.

[35] A. Alamin, "The Role of Red Blood Cells in Hemostasis," *Semin. Thromb. Hemost.*, vol. 47, pp. 26–31, 2021, doi: 10.1055/s-0040-1718889.